Journal of Visualized Experiments

Evaluation of an Exclusive Spur Dike U-Turn Design with Radar-Collected Data and Simulation

--Manuscript Draft--

Article Type:	Invited Methods Article - Author Produced Video
Manuscript Number:	JoVE60675R4
Full Title:	Evaluation of an Exclusive Spur Dike U-Turn Design with Radar-Collected Data and Simulation
Section/Category:	JoVE Engineering
Keywords:	U-turn; spur dike; VISSIM; traffic data; traffic congestion; transportation; highway
Corresponding Author:	Yang Shao Chang'an University Xi'an, Shaanxi CHINA
Corresponding Author's Institution:	Chang'an University
Corresponding Author E-Mail:	shaoyang19901015@outlook.com
Order of Authors:	Yang Shao
	Hongtao Yu
	Huan Wu
	Xueyan Han
	Xizhen Zhou
	Christian G. Claudel
	Hualing Zhang
	Chen Yang
Additional Information:	
Question	**Response**
Please indicate whether this article will be Standard Access or Open Access.	Standard Access (US$1200)

TITLE:

Evaluation of an Exclusive Spur Dike U-Turn Design with Radar-Collected Data and Simulation

AUTHORS AND AFFILIATIONS:

Yang Shao[1], Hongtao Yu[1], Huan Wu[2], Xueyan Han[1], Xizhen Zhou[1], Christian G. Claudel[3], Hualing Zhang[4], Chen Yang[5]

[1]Highway Academy, Chang'an University, Xi'an, Shaanxi, China
[2]Human Resource Department, Xi'an Shiyou University, Xi'an, Shaanxi, China
[3]Cockrell School of Engineering, University of Texas at Austin, Austin, TX, USA
[4]Department of Earth and Atmospheric Science, University of Houston, Houston, TX, USA
[5]School of Foreign Languages, Xi'an Shiyou University, Xi'an, Shaanxi, China

Corresponding Author:

Yang Shao (shaoyang19901015@outlook.com)

Email Addresses of Co-Authors:

Hongtao Yu (yu-hongtao@qq.com)
Huan Wu (285383575@qq.com)
Xueyan Han (975066967@qq.com)
Xizhen Zhou (zhouxizhen@chd.edu.cn)
Christian G. Claudel (christian.claudel@utexas.edu)
Hualing Zhang (hzhang67@uh.edu)
Chen Yang (511544867@qq.com)

KEYWORDS:

U-turn, spur dike, simulation, traffic data, traffic congestion, transportation, highway

SUMMARY:

This protocol describes the process of solving a microscopic traffic problem with simulation. The whole process contains a detailed description of data collection, data analysis, simulation model build, simulation calibration, and sensitive analysis. Modifications and troubleshooting of the method are also discussed.

ABSTRACT:

Traditional U-turn designs can improve operational features obviously, while U-turn diversions and merge segments still cause traffic congestion, conflicts, and delays. An exclusive spur dike U-turn lane design (ESUL) is proposed here to solve the disadvantages of traditional U-turn designs. To evaluate the operation performance of ESUL, a traffic simulation protocol is needed. The whole simulation process includes five steps: data collection, data analysis, simulation model build, simulation calibration, and sensitive analysis. Data collection and simulation model build are two critical steps and are described later in greater detail. Three indexes (travel time, delay, and number of stops) are commonly used in the evaluation, and other parameters can be measured from the simulation according to experimental needs. The results show that the ESUL

significantly diminishes the disadvantages of traditional U-turn designs. The simulation can be applied to solve microscopic traffic problems, such as in single or several adjacent intersections or short segments. This method is not suitable for larger scale road networks or evaluations without data collection.

INTRODUCTION:

Some traffic problems, such as traffic congestion at an intersection or short segment, can be solved or improved by optimizing the road design, change signal timing, traffic management measurements, and other transportation technologies[1-4]. These improvements either have a positive or negative effect on traffic flow operations compared to the original situations. The changes in traffic operations can be compared in traffic simulation software rather than in actual reconstruction of the intersection or segment. The traffic simulation method is a quick and cheap option when one or more improvement plans are proposed, especially when comparing different improvement plans or evaluating the effectiveness of improvements. This article introduces the process of solving a traffic problem with simulation by evaluating traffic flow operational features of an exclusive spur dike U-turn lane design[5].

U-turn movement is a widespread traffic demand that requires a U-turn median opening on the road, but this has been debated. Designing a U-turn opening can cause traffic congestion, while closing the U-turn opening can cause detours for the U-turn vehicles. Two movements, U-turn vehicles and direct left-turn vehicles, require a U-turn opening and cause traffic delays, stops, or even accidents. Some technologies have been proposed to solve the disadvantages of U-turn movements, such as signalization[6,7], exclusive left turn lanes[8,9], and autonomous vehicles[10,11]. Improvement potential still exists on U-turn issues, due to the above solutions having restrictive applications. A new U-turn design may be a better solution under certain conditions and be able to address existing problems.

The most popular U-turn design is the median U-turn intersection (MUTI)[12-15], as shown in **Figure 1**. A significant limitation of the MUTI is that it cannot distinguish U-turn vehicles from passing vehicles and that traffic conflict still exists[16,17]. A modified U-turn design called the exclusive spur dike U-turn lane (ESUL; **Figure 2**) is proposed here and aims to diminish traffic congestion by introducing an exclusive U-turn lane on both sides of a median. The ESUL can significantly reduce travel time, delays, and the number of stops due to its channelization of the two flows.

To prove that the ESUL is more efficient than the normal MUTI, a rigorous protocol is needed. The ESUL cannot be actually constructed before a theoretical model; thus, simulation is needed[18]. Using traffic flow parameters, some key models have been used in simulation research[19], such as driving behavior models[20,21], car following models[22,23], U-turn models[4], and lane change models[21]. The accuracy of traffic flow simulations is widely accepted[16,24]. In this study, both the MUTI and ESUL are simulated with collected data to compare improvements made by the ESUL. To guarantee accuracy, a sensitive analysis of the ESUL is also simulated, which can apply to many different traffic situations.

This protocol presents experimental procedures for solving real traffic problems. The methods

for traffic data collection, data analysis, and analysis of overall efficiency of traffic improvements are proposed. The procedure can be summarized in five steps: 1) traffic data collection, 2) data analysis, 3) simulation model build, 4) calibration of simulation model, and 5) sensitivity analysis of operational performance. If any one of these requirements in the five steps is not met, the process is incomplete and insufficient to prove effectiveness.

PROTOCOL:

1. Preparation of the equipment

1.1. Prepare two of each of the following devices to collect two-direction traffic flows: radars, laptops, batteries and cables for radars and laptops, cameras, and radar and camera tripods.

NOTE: The radar and its corresponding software are used to collect vehicle speed and trajectory, and this is more accurate than a speed gun. The radar is not the only choice if other equipment is available for collecting vehicle speed, trajectory, and volume. As radar signals can be easily blocked by large vehicles, videos shot by cameras can be used for vehicle counting. During the investigation, if the weather is rainy or sunny, protection of the equipment is needed. Especially on a sunny day, the equipment may reach a high temperature and shut down, so an umbrella or cooling equipment is needed for this situation.

2. Testing of the equipment

2.1. Ensure that all investigators are wearing reflective vests.

2.2. Prepare the radar tripod and extend it as tall as possible. Set the tripod taller than 2 m to avoid signals from being blocked on the roadside.

2.3. Install the radar on top of the tripod and lock the radar.

2.4. Set the radar about 0.5 m next to the roadside, adjust the radar vertically, and face the vehicle direction or opposite direction. Keep the angle between the road and radar as small as possible.

NOTE: The radar can detect 200 m at most. If the radar is set too close to the lane, it may blow over the passing vehicles. Thus, 0.5−1.0 m is the usual distance to the lane.

2.5. Turn on the power battery and connect the laptop to the power battery. Plug in the radar power cable and plug in the radar data USB to the laptop. When all cables are connected, turn on the laptop.

2.6. Set the camera next to the radar to shoot the vehicle flow.

2.7. Opening the radar software

2.7.1. Click **Communication check**, then select the radar ID number from the dropdown list. It will show **Radar Detected** with an ID number.

2.7.2. Click **Investigation setup**. In the pop-up menu, click **Read RLU time**, and the **Device time** on the left will change. Then, click **Set up RLU time**, and **PC current time** on the left will also change.

2.7.3. Click **Start investigation**, and the device working status will change from **Data recording is not proceeding** and **No data in device** to **Data recording in proceeding** and **Data in device**. Click **Close** to close this dialog box.

2.7.4. Click the **Realtime view** to check the radar status. A new dialog box will show, and the radar data will be rolled quickly. This means that the radar is detecting the vehicles and works well. Keep this dialog box open until the collection is finished.

NOTE: The vehicle can be captured by the radar when passing the radar.

2.7.5. Click **Close** on the dialog box to finish the collection.

2.7.6. Click **Investigation setup** | **End investigation**, and confirm in the dialog box. Click the **Close** button.

2.7.7. Select **Data download** in the main menu. Click **Browse** to select a place to save the radar data. Input an individual name for the spreadsheet. Click the **Start download** button, a progress bar will show, and a dialog box will appear after downloading. Click **Confirm** to finish data collection.

2.7.8. Click **Investigation setup** | **Erase data record**, and confirm it in the next dialog box to clear the internal memory of the radar.

NOTE: A test of all equipment is needed before departure to the data collection location. Move all the equipment to the data collection location if all the parts work well.

3. Data collection

3.1. Selection of data collection location (**Figure 3**)

3.1.1. Select a suitable location that is similar to the intersection type used in the research.

NOTE: This is the key requirement in location selection. The shape of the location, traffic flow situation, traffic light control, and other controls are all needed in consideration. The more similar the study site, the more accurate the results. A U-turn median opening on the freeway is needed. A sufficiently long line of sight and clearance are required, which is necessary for radar and safety

for investigators. Based on the detect distance of the radar and vehicle stop distance, the line of sight should be at least 200 m from the location to an upstream direction.

3.1.2. Check the clearance of the radar direction. Make sure that there are no trees, shrubs, footbridges, traffic signs or streetlights in sight.

3.1.3. Ensure that the location is a safe place for the equipment and investigators. Whether the equipment is set on the roadside or above the road depends on the terrain.

3.1.4. Place the equipment in a secluded place to avoid gaining the driver's attention.

NOTE: According to prior experience, some drivers may slow down if they see the investigation equipment, which will lead to errors. The data acquisition equipment can be regarded as a measuring device for traffic police to measure speeding vehicles.

3.2. Collection of traffic data

3.2.1. Choose the collection time.

3.2.1.1. Collect 3 h of data: 1 h in morning peak, 1 h at noon valley, and 1 h at evening peak.

3.2.1.2. Check the accurate peak and valley time from the traffic research report, traffic police department, or traffic business companies[25,26] (**Figure 4**).

NOTE: If there is no traffic report or analysis as reference, collect 3 h of data during the three periods mentioned above, and choose the highest data.

3.2.1.3. Input the data with highest traffic volume over a 1 h period into the simulation model and analysis section. Use the remaining 2 h of data for verification at the end.

3.2.2. Setup of the equipment

3.2.2.1. Adjust the radar direction, and set the camera next to the radar where it can capture all lanes. Repeat the process of installing all equipment in section 2 on the pedestrian bridge.

NOTE: The clearance before the radar should be as long and wide as possible to cover the whole range of U-turn movements. The EW (east to west) radar faces the traffic flow, and the WE (west to east) radar faces towards the vehicle tails due to road alignment (**Figure 5**). There are no differences between results from setting up the equipment on the inner vs. outer side of the lanes. The inner or outer side of the radar location only affects the coordinate system of trajectory figures with radar data. When the radar faces traffic flow, the detected running speed is negative and needs to be reversed during data processing. When the radar faces traffic flow, the detected running speed is positive and can be used directly.

3.2.2.2. Set the radars and cameras so that they are slightly taller than the bridge railings to ensure clearance before the radars and cameras.

NOTE: There is no need for the radars to be as tall as the roadside settlement.

3.2.3. Ensure that the timing of the radars, laptops, and cameras are consistent with real-time.

3.2.4. Start two radars and cameras simultaneously to schedule time.

3.2.5. Check whether the radars and cameras work normally every 5 min during data collection to ensure that all parts work well.

3.2.6. End the data collection and output the radar data as a spreadsheet with an identified name (**Table 1**).

4. Data analysis

4.1. Using calculation software to extract the radar data and draw operating speed and trajectories figures from the spreadsheet.

NOTE: X/Y coordinates and X/Y speed are in the spreadsheet.

4.2. Delete obviously discrete points in the figures. These points are radar errors.

NOTE: The radar detects a large range of area, so the data may contain target vehicles, opposite vehicles, and non-motor vehicles in non-motor vehicle lanes. When plotting all data as figures, the three-lane target vehicles are obvious, and the remaining points are “obviously discrete points”. The detection areas are straight in **Figure 3**, the width of the three lanes is known, and the “obviously discrete points” can be deleted in the software. Plot the necessary points as shown in **Figure 6b,d**.

4.3. Replay the traffic videos and count manually to obtain the traffic volume and types.

NOTE: Vehicles can be divided into cars and trucks according to size. All cars, taxies, and small trucks within 6 m are classified here as cars. All large trucks and buses are classified as trucks.

4.4. Select the highest traffic volume group as representative data and input it into the simulation described in section 5.

NOTE: Only one group of data is needed in the simulation and sensitivity analysis. Data from the other two groups will be simulated as verification.

5. Building the simulation model

5.1. Building of the road

5.1.1. Open the simulation software. Click **Map** button at the top of the interface and zoom in the map to find the data collection location.

5.1.2. Click **Links** on the left, then move the cursor to the start location of the link, and right-click. Select **Add New Link**, input the link name and number of lanes, and click **OK**. Drag the cursor to draw the link on the map.

5.1.3. Right click the link and select **Add Point**. Add points and drag points to make the link smoother with real road alignment in the map.

5.1.4. Repeat steps 5.1.2 and 5.1.3 3x to build four segments, except for the U-turn median opening.

5.1.5. Hold the right button of the mouse and **Ctrl** button on the keyboard, then drag the endpoint of one link to the adjacent link to connect the links. This part is called the "connector" and can be smoother as more points are added.

5.1.6. Repeat step 5.1.5 to connect all links and U-turn routes.

5.2. Input of the desired speed

5.2.1. Select **Base Data** from the top bar, then select **Distributions** | **Desired speed**.

5.2.2. Click the green-cross **Add** button at the bottom to add a new desired speed, then name it.

5.2.3. In the **Desired Speed Distributions** dialog box, input the maximum speed collected from the representative data as the maximum desired speed, then input the average speed calculated from the representative data as the minimum desired speed. Delete the default data.

5.2.4. Input a name for this desired speed, which is usually named using a direction.

5.2.5. Repeat steps 5.2.3 and 5.2.4 to build all desired speeds (WE, EW, WW U-turn, and EE U-turn).

5.3. Vehicle composition

5.3.1. Select the **Lists** button from the top bar, then click **Private Transport** | **Vehicle Compositions**.

5.3.2. Click the green-cross **Add** button at the bottom to add a new vehicle composition. Select the desired speed built in step 5.2 as **Car**.

5.3.3. Click the green-cross **Add** button to add the vehicle type bus/truck as **HGV**. Select the same desired speed as done in step 5.3.2.

5.3.4. Input the volume of cars and trucks at **RelFlow** from the representative data.

5.3.5. Repeat steps 5.3.2–5.3.5 to build all vehicle compositions (WE, EW, WW U-turn, and EE U-turn).

5.4. Vehicle routes

5.4.1. Select **Vehicle Route** from the left menu bar.

5.4.2. Move the cursor to the upstream of one link as the start point, right-click, then select **Add New Static Vehicle Routing Decision**.

5.4.3. Drag the blue cursor representing the vehicle routes in data collection. Repeat this step 4x in WE, EW, WW U-turn, and EE U-turn to draw all vehicle routes.

5.5. Reduced speed areas

5.5.1. Select **Reduced Speed Areas** from the left menu bar.

5.5.2. Right-click at the upstream of U-turn opening, then select **Add New Reduced Speed Area**.

NOTE: The length of the area depends on the representative data and speed change length.

5.5.3. Build this area in both directions.

5.6. Conflict areas

5.6.1. Select **Conflict Areas** from the left menu bar. Four yellow conflict areas will be shown in the median opening section.

5.6.2. Right-click one yellow conflict area and select **Set Status to Undetermined** as the realistic situation and conflict areas turn red.

5.6.3. Repeat step 5.6.2 for all four conflict areas.

5.7. Travel time measurement

5.7.1. Select **Vehicle Travel Times** from the left menu bar.

5.7.2. Right-click at the beginning of one link and select **Add New Vehicle Travel Time Measurement**.

5.7.3. Drag the cursor to the end of the link to build the one vehicle travel time measurement. Repeat this step for all vehicle routes (WE, EW, WW U-turn, and EE U-turn).

5.7.4. Name each travel time measurement with the corresponding direction.

NOTE: To compare the operating situations with improvement designs, the length of the travel time measurements needs to be the same in both simulation models.

5.8 Vehicle input

5.8.1 Select **Vehicle Inputs** from the left menu bar. Click the starting point of one link and right click to add new vehicle input.

5.8.2 Move the mouse to left bottom and input volume from representative data. Repeat this step for all links.

5.9 Build another ESUL simulation model as comparison, only the U-turn opening part needs to be modified (**Figure 7** and **Table 2**).

5.10 Click the blue play button at the top of the interface, and the simulation will start. Drag the scale at the left of the play button, which can adjust the simulation speed.

NOTE: The instrument button **Quick mode** can make the simulation speed to the maximum.

5.11 When the simulation ends, all results will be shown at the bottom of the interface. Copy the results into a new spreadsheet. Here, travel time, delay, and the number of stops are evaluated in the analysis[27].

6. Simulation model calibration

6.1. Input the traffic volume of the representative data into simulation software and perform the simulation (**Figure 8a**).

6.2. Compare the traffic volume from the simulation results with the collected data volume.

6.3. Calculate the capacity using **Equation 1** below:

$$C = \frac{3600}{h_t} \quad (1)$$

where C denotes the ideal capacity (veh/h) and h_t denotes the average minimum headway (s).

6.4. Using the capacity, estimate the simulation error as the mean absolute percent error (MAPE)

following **Equation 2**:

$$MAPE = \frac{1}{n}\sum_{i=1}^{n}\left|\frac{C_v^i - C_f^i}{C_f^i}\right| \quad (2)$$

where n denotes the four different flows in this study, C_v^i is the capacity simulated in the simulation model (veh/h), and C_f^i is the capacity of the investigation (veh/h). The calculated MAPE is presented in **Table 3**.

NOTE: The simulation model can be used if the MAPE is small[28-30].

6.5. Modify the parameters (i.e., random seed, car follow model type, lane change rule, etc.) based on instructions of the simulation software, or check all steps described above when building the simulation model[31-34].

7. Sensitivity analysis

NOTE: Sensitivity analysis process is shown in **Figure 8b**. The collected data can only reflect its own performance (**Figure 9**, **Table 4**, **Table 5**, and **Table 6**). To prove the effectiveness under all situations, all possible traffic situations and different combinations were input into the simulation model to ensure that all situations are covered between the MUTI and ESUL (**Figure 10** and **Table 7**).

7.1. Select the car/truck (bus) ratio and operating speed of the representative data. Maintain these parameters.

7.2. Set the U-turn ratio from ~0.03–0.15 in the sensitivity analysis with an increase of 0.03, which means five U-turn ratios in the sensitivity analysis.

NOTE: According to the representative data in **Table 1**, the range of the U-turn rate is 0.04–0.15.

7.3. Set traffic volume from ~0.2–1.0 V/C with an increase of 693 veh/h (0.1 V/C; **Table 7**)**,** which means nine volumes in the sensitivity analysis.

NOTE: The maximum traffic volume is 6,930 veh/h in an urban freeway with a three-lane segment, corresponding to service level E according to the AASHTO's Highway Capacity Manual[35] when the design speed is 80 km/h.

7.4. Simulate all 45 situations and save the results in both the present situation (MUTI) and improved situation (ESUL).

7.5. Verify improvements in travel time and delays by calculating the ratio = (MUTI - ESUL)/MUTI x 100%. Verify improvements in the number of stops by calculating reduced time = MUTI - ESUL.

NOTE: In the final results (**Figure 10**), a positive (>0) result means that the ESUL improved the traffic situation, while a negative (<0) result in sensitivity represents the opposite.

REPRESENTATIVE RESULTS:

Figure 2 shows the illustration of the ESUL for U-turn median opening. WENS mean four cardinal directions. The main road has six lanes with two directions. Greenbelts divide non-motorized lane on both sides and divide the two directions in the middle. Flow 1 is the east to west through traffic, flow 2 is east to east U-turn flow, flow 3 is west to east through traffic, and flow 4 is west to west U-turn traffic.

The functions of the inner 2 lanes of the ESUL are to divert, decelerate, U-turn, accelerate, look for headway, and merge the U-turn vehicles. The spur dike part is the core part and is different from ordinary U-turn designs. This part has the potential to force traffic flow to move outward slightly (one-lane width) and separate the through-traffic and U-turn traffic after the spur dike.

The spur dike design has three significant differences. First, it provides a specific U-turn lane to avoid influence from through traffic by moving the whole lanes outward. Compared to the markings, drivers cannot across the spur dike and must follow the lanes to divide the two flows apart[36,37]. Second, it maximally uses the land by symmetrically designing both two-direction U-turn demands. Third, the spur dike adjusts different U-turn radii of vehicles and uses the land flexibly.

Figure 3 shows the data collection location, which is a typical median opening at the northwest corner of the second loop road of Xi'an City in Shaanxi Province, China. The loop road in this research consists of six lanes, and the speed limitation in the loop road is 80 km/h (**Figure 3a**). The width of the lane is 3.5 m and median width is 1.2 m on average. The median opening section is 10 m wide and 17 m long. Two non-motor vehicle lanes (9 m width) are on both sides, and a 1.5 m greenbelt divides them from the main lanes (**Figure 3b**).

The distance between the upstream and downstream interchanges near the median opening is 5.1 km (**Figure 3a**). Since there is no entrance or exit for this section, the operation speed can reach the speed limit after the median opening reaches 200 m. From the median opening, it is 1.4 km to the upstream interchange and 3.6 km to the downstream interchange. Vehicles make a detour of 10 km (delay of 9 min at most) if no U-turn opening is designed. U-turn vehicles must wait for a long time when meeting at the intersection or are forced to join, resulting in delays or stopping of through-traffic. **Figure 4** shows that the morning peak appears from 7:00 A.M. to 9:00 A.M., the evening peak appears from 17:00 to 19:00, and the valley (excluding late night) appears from 12:00 to 14:00.

The speeds of all traffic from east to west are shown in **Figure 6a**. The U-turn opening occurs at ~70 m at the horizontal axis. The deceleration and acceleration are obvious near 70 m, which indicates that the vehicles were affected by U-turn vehicles. The peak value in **Figure 6a** is under 80 km/h, and points are mainly centralized under 40 km/h, which indicate that the operating

speed was much lower than the speed limit (80 km/h). **Figure 6b** shows the trajectories of traffic flow from east to west. The three lanes and U-turn vehicles trajectories are identified easily in the figure. The lowest trajectory is dark blue and wider than the two trajectories above it, indicating merging between the U-turn vehicles and through vehicles. The merging movement starts at 60 m and ends at 40 m, which represents a 20 m merge segment. The through-traffic in the inner lane was affected seriously by U-turn vehicles.

Figure 6c is the speed of flows from west to east. When the running speed reaches 80 m at the U-turn opening, it starts to increase. The result indicates that the WW U-turn flow had a smaller influence on WE via flow that was due to diversion movement (rather than merge movement; **Figure 6b**. The points starting from 0 km/h indicate that the WW U-turn vehicles caused stops and deceleration for whole vehicles. **Figure 6d** shows the trajectories from west to east of through-traffic and U-turn traffic. The U-turn section has high trees, which block the radar signals for detecting U-turn movements.

Figure 7 shows one-half of the ESUL design. Lanes 1 and 4 are through-traffic lanes, and lanes 2 and 3 are U-turn lanes. The calculation of each section is based on previously published guidelines[35,38] and studies[39,40]. Section AB is based on a road alignment process, section BC is dependent on the drivers' reaction times and movement procedures, section CD is the diversion part, and section DE contains deceleration and safety distance. Section EF provides enough space to U-turn. Section FH and HI contain acceleration, headway finding, and combined motion separately. All sections are described in **Table 2** according to a design speed of 80 km/h.

Figure 10a shows that the flow 1 travel time ratio decreased with ESUL under all traffic combinations within 20%–40%. The delay greatly decreased by 35%−70% (**Figure 10b)**. The number of stops decreased slightly, with a maximum value of 0.4 (**Figure 10c**). The ESUL showed a significant improvement for EW through-traffic in all situations. **Figure 9e,f** and **Figure 10d** show the sensitivity results of flow 2 (EE U-turn vehicles). All three indexes of EE U-turn vehicles were improved greatly. The travel time shown in **Figure 10d** decreased by 20%–70% with increasing traffic volume. The delays in **Figure 10e** decreased more than the travel time and reached nearly 100% at the peak value. The minimum improvement ratio was larger than 70%. A significant improvement for number of stops shown in **Figure 10f** reached six at most.

Figure 9i,j and **Figure 10h** show the sensitivity results of flow 3 (WE through vehicles). With a similar trend to flow 1, flow 3 improved a lot with ESUL. Travel time decreased by 40%–50% in **Figure 10h**. Delays decreased by 50%–90% in **Figure 10i**. The number of stops only decreased 0.4x at most in **Figure 10j**. In flow 4, the WW U-turn vehicles and sensitivity results are shown in **Figure 9l,m** and **Figure 10k**. The travel time decreased by ~20%–60% with traffic volume increases (**Figure 10k**). In **Figure 10l**, delays increased 1% when traffic volume was 1,386 veh/h, and the U-turn ratio was 0.06. Delays decreased significantly by 54%–97% in the rest scope. The number of stops decreases up to 6x at most (**Figure 10m**).

FIGURE AND TABLE LEGENDS:

Figure 1: Examples of median U-turn intersections (**MUTIs**)**.** Two designs represent the common

U-turn opening on the road, but it should be noted that the U-turn vehicles may cause traffic conflicts with passing vehicles, whether in the same or opposite direction flow.

Figure 2: Illustration of the ESUL design on provincial trunk highway. W = west, E = east, N = north, S = south.

Figure 3: Data collection location at a median at the northwest corner second loop road in Xi'an. Coordinates: 108.903898, 34.301482. (**a**) The investigation location schematic. (**b**) The MUTI of the U-turn median opening. The image was taken by a drone at the height of 150 m.

Figure 4: 24 h congestion index. (**a**) The 24 h congestion trend of major cities from 2015 to 2017[25]. (**b**) The 24 h congestion delay index for Xi'an on May 22nd, 2019[25,26]. The data in panel a comes from the 2017 Traffic Analysis Reports for Major Cities in China[25], which is provided by a Chinese web mapping navigation provider[41]. The data in panel b comes from the real-time congestion index in Xi'an on May 22nd, 2019[26].

Figure 5: Data collection with radar on a pedestrian bridge at the U-turn location.

Figure 6: Speed and trajectories of traffic flows: (**a**) Speed of vehicles from east to west. (**b**) Trajectories of vehicles from east to west. (**c**) Speed of vehicles from west to east. (**d**) Trajectories of vehicles from west to east.

Figure 7: Geometry of ESUL design. The blue arrow represents vehicles traveling straight through, and the red arrow represents U-turn vehicles.

Figure 8: Flowchart of calculating MAPE and sensitive analysis. (**a**) Calculation process of MAPE. (**b**) Process of sensitive analysis.

Figure 9: Comparison between MUTI and ESUL with collected data. Comparison of travel time (**a**), delay (**b**) and number of stops (**c**) with morning peak (h). Comparison of travel time (**d**), delay (**e**) and number of stops (**f**) with middle noon valley (h). Comparison of travel time (**h**), delay (**i**) and number of stops (**j**) with evening peak (h).

Figure 10: Sensitivity analysis of all flows, including EW through, EE U-turn, WE through and WW U-turn. X-axis = different traffic volumes, Y-axis = U-turn ratio, and Z-axis = improvement ratio (ratio = [MUTI – ESUL]/MUTI x 100%) in travel time and delay, reduced times (reduced times = MUTI - ESUL) in number of stops. (**a-c**) EW through flow, (**d-f**) EE U-turn flow, (**h-j**) WE through flow, and (**k-m**) WW U-turn flow. Every three figures are travel time (**a,d,h,k**), delay (**b,e,i,l**) and the number of stops (**c,f,j,m**), respectively.

Table 1: Collected vehicle information. A minimum speed of 0 km/h indicates that some vehicles were stopped before starting to move.

Table 2: Geometric parameters of ESUL. The calculation of each section is based on previously

published guidelines[35,38] and studies[39,40]. The value in **Table 2** is input into the simulation model to evaluate ESUL performance at a design speed of 80 km/h.

Table 3: Simulation calibration results. Calibration between the investigation and simulation is shown in the table. The MAPE is calculated using Equation 2, and the results are acceptable[27,30].

Table 4: Simulation results of MUTI and ESUL with morning peak data. In the morning peak, the ESUL improves significantly more than the MUTI. Travel time decreased by 29.4%−57.5%. Delay decreased by 44.4%−97.7%. The number of stops is completely diminished.

Table 5: Simulation results of MUTI and ESUL with middle noon data. At noon, the travel time decreased by 31.3%–43.8%. Delay decreased by 50.0%–87.1% and no number of stops exist with ESUL.

Table 6: Simulation results of MUTI and ESUL with evening peak data. With the evening peak data, travel time decreased by 27.7%−56.6%. Delay decreased by 60.7%−91.8%. The number of stops also diminishes with the ESUL.

Table 7: Parameters input into sensitivity analysis in simulation.

DISCUSSION:

In this article, the procedure of solving a traffic problem at an intersection or short segment using simulation was discussed. Several points deserve special attention and are discussed in more detail here.

Field data collection is the first thing deserving attention. Some requirements for data collection location are as follows: 1) Finding a suitable location for data collection. The location should be similar to the road geometric shape in the study, which is the premise of data collection. 2) Determination of the set location of radar and other equipment by finding an enough clearance, where radar signals cannot be blocked. Some state-of-art technologies can be used, such as drones, to detect traffic operations. The entire observation area should be clear of barriers, like trees or architecture. 3) Finally, the data collection time should be at least 3 h in one location. The time should reflect the morning and evening peaks as well as the valley situation in the day. The time of congestion index can be obtained from observation or from another reliable transportation publisher.

Simulation model building is another critical step. The accuracy of the simulation model will lead to different simulation errors. The first thing in the simulation model is the connector. If one link on one side of the connector moves, the connector may be out of shape and intrude the adjacent link or connector, which may result in errors. So, it is important to recalculate the connector whenever moving a link is necessary.

Another key step is the conflict rule in conflict area. Use conflict areas instead of priority rules to simulate the right of way at intersections. Compared to priority rules, conflict areas are

automatically displayed, and therefore are easier to edit and better reflect the driving behavior. The conflict rule should be the same as data collection, and every conflict area should be set with corresponding rules. The last critical step is adjustment of the parameters regarding driving behaviors when simulation error (MAPE) is big. Driving behaviors have several individual parameters, and a small change in each parameter may lead to a positive or negative impact on the results. It is key to adjust the various parameters carefully and repeatedly.

Usually, the travel time, delay and the number of stops is most common used indexes in evaluating the operational features in simulation. Many other indexes can also be obtained from the simulation (i.e., vehicle volume, exhaust emission, fuel consumption, pedestrian record, safety evaluation, vehicle behaviors, vehicle routes, coordinates, etc.). It is important to select the corresponding evaluation indexes according to the different experimental needs. Other indexes, except the three above that are most commonly used, may lead to new research findings or methods.

Using “quick mode” when performing the simulation may allow the simulation to reach the highest speed and save time, especially during the sensitive analysis. Thus, dozens of simulations are needed. The simulation result stays the same no matter which simulation speed is chosen.

There are two major areas for future applications. One application is the solving of traffic problems and evaluating one or more traffic designs at an intersection or short segment. The simulation helps to evaluate microscopic traffic behaviors, whether it includes vehicles, pedestrians, infrastructure modifications, or traffic management measurements. Second, the process provides a sufficient practice guide for those conducting traffic research. The provisions help to obtain accurate and robust data on traffic simulation measurements.

This method also has some limitations. First, the radar can detect a straight direction, and this requires that the target segment is also straight. The radar cannot be used for curved segments, like ramps. Second, the radar requires sufficient clearance to detect the vehicles. However, in the real environment, there are always trees or billboards that block the signal. It is difficult to find a suitable place for radar settlement. In addition, when the traffic volume is large or vehicles are close to each other, radar cannot distinguish the vehicles, and counting manually from the video is the only option, which is a lot of work. Efficiency and accuracy can be improved if the protocol also uses a method that can count and classify vehicles automatically.

ACKNOWLEDGMENTS:
The authors would like to acknowledge the China Scholarship Council for partially funding this work was with the file No.201506560015.

DISCLOSURES:
The authors have nothing to disclose.

REFERENCES:

1. Tang J. Q., Heinimann H. R., Ma, X. L. A resilience-oriented approach for quantitatively assessing recurrent spatial-temporal congestion on urban roads. *PLoS ONE*. **13** (1), e0190616 (2018).
2. Bared, J. G., Kaisar, E. I. Median U-turn design as an alternative treatment for left turns at signalized intersections. *ITE Journal*. **72** (2), 50-54 (2002).
3. El Esawey, M., Sayed, T. Operational performance analysis of the unconventional median U-turn intersection design. *Canadian Journal of Civil Engineering*. **38** (11), 1249-1261 (2011).
4. Leng, J., Zhang, Y., Sun, M. VISSIM-based simulation approach to evaluation of design and operational performance of U-turn at intersection in China. *2008 International Workshop on Modelling, Simulation and Optimization. IEEE*. Hong Kong, China (2008).
5. Shao Y. et al. Evaluating the sustainable traffic flow operational features of an exclusive spur dike U-turn lane design. *PLoS ONE*. **14** (4), e0214759 (2019).
6. Zhao, J., Ma, W. J., Head, K., Yang, X. G. Optimal Intersection Operation with Median U-Turn: Lane-Based Approach. *Transportation Research Record*. (2439), 71-82 (2014).
7. Hummer J. E., Reid, J. E. Unconventional Left Turn Alternatives for Urban and Suburban Arterials-An Update. *Urban Street Symposium Conference Proceedings*. Dallas, TX (1999).
8. Ram, J., Vanasse, H. B. Synthesis of the Median U-Turn Intersection Treatment, Safety, and Operational Benefits. *Transportation Research Board*. Washington, DC (2007).
9. Levinson, H. S., Koepke, F. J., Geiger, D., Allyn, D., Palumbo, C. Indirect left turns-the Michigan experience. *Fourth Access Management Conference.* Portland, OR (2000).
10. Mousa, M., Sharma, K., Claudel, G. C. Inertial Measurement Units-Based Probe Vehicles: Automatic Calibration, Trajectory Estimation, and Context Detection. *IEEE Transactions on Intelligent Transportation Systems.* 1-11 (2017).
11. Odat, E., Shamma, J., Claudel, G. C. Vehicle Classification and Speed Estimation Using Combined Passive Infrared/Ultrasonic Sensors. *IEEE Transactions on Intelligent Transportation Systems*. 1-14 (2017).
12. Liu, P. et al. Operational effects of U-turns as alternatives to direct left-turns. *Journal of Transportation Engineering*. **133** (5), 327-334 (2007).
13. Potts, I. B. et al. Safety of U-turns at Unsignalized Median Opening. *Transportation Research Board*. Washington, DC (2004).
14. Yang, X. K., Zhou, G. H. CORSIM-Based Simulation Approach to Evaluation of Direct Left Turn vs Right Rurn Plus U-Turn from Driveways. *Journal of Transportation Engineering*. **130** (1), 68-75 (2004).
15. Guo, Y. Y., Sayed, T., Zaki, M. H. Exploring Evasive Action-Based Indicators for PTW Conflicts in Shared Traffic Facility Environments. *Transportation Engineering, Part A: Systems*. **144** (11), 04018065 (2018).
16. Liu, P., Qu, X., Yu, H., Wang, W., Gao, B. Development of a VISSIM simulation model for U-turns at unsignalized intersections. *Journal of Transportation Engineering*. **138** (11), 1333-1339 (2012).
17. Shao, Y., Han, X. Y., Wu, H., Claudel, G. C. Evaluating Signalization and Channelization Selections at Intersections Based on an Entropy Method. *Entropy*. **21** (8), 808 (2019).
18. Ander, P., Oihane, K. E., Ainhoa, A., Cruz, E. B. Transport Choice Modeling for the Evaluation of New Transport Policies. *Sustainability*. **10** (4), 1230 (2018).

698 19. Wang, J., Kong, Y., Fu, T., Stipanicic, J. The impact of vehicle moving violations and freeway
699 traffic flow on crash risk: An application of plugin development for microsimulation. *PLoS ONE.*
700 **12** (9), e0184564 (2017).
701 20. Lin, C., Gong, B., Qu, X. Low Emissions and Delay Optimization for an Isolated Signalized
702 Intersection Based on Vehicular Trajectories. *PLoS ONE*. **10** (12), e0146018 (2015).
703 21. Tang, T. Q., Wang, Y. P., Yang, X. B., Huang, H. J. A multilane traffic flow model accounting for
704 lane width, lanechanging and the number of lanes. *Networks and Spatial Economics*. (14), 465-
705 483 (2014).
706 22. Gupta, A. K., Dhiman, I. Analyses of a continuum traffic flow model for a nonlane-based
707 system. *International Journal of Modern Physics C*. **25** (10), 1450045 (2014).
708 23. Chen, H., Zhang, N., Qian, Z. VISSIM-Based Simulation of the Left-Turn Waiting Zone at
709 Signalized Intersection. *2008 International Conference on Intelligent Computation Technology*
710 *and Automation (ICICTA)*. IEEE. Hunan, China (2008).
711 24. PTV AG. *PTV VISSIM 10 User Manual*. Karlsruhe, Germany (2018).
712 25. AutoNavi Traffic Big-data. *2017 Traffic Analysis Reports for Major Cities in China*.
713 https://report.amap.com/share.do?id=8a38bb86614afa0801614b0a029a2f79 (2018).
714 26. AutoNavi Traffic Big-data. *Xi'an realtime traffic congestion delay index.*
715 https://trp.autonavi.com/detail.do?city=610100 (2019).
716 27. Xiang, Y. et al. Evaluating the Operational Features of an Unconventional Dual-Bay U-Turn
717 Design for Intersections. *PLoS ONE*. **11** (7), e0158914 (2016).
718 28. Kuang, Y., Qu, X., Weng, J., Etemad, S. A. How Does the Driver's Perception Reaction Time
719 Affect the Performances of Crash Surrogate Measures? *PLoS ONE*. **10** (9), e0138617 (2015).
720 29. Zhao, F., Sun, H., Wu, J., Gao, Z., Liu, R. Analysis of Road Network Pattern Considering
721 Population Distribution and Central Business District. *PLoS ONE*. **11** (3), e0151676 (2016).
722 30. Jian S. *Guideline for microscopic traffic simulation analysis*. Tongji University Press. Shanghai,
723 China (2014).
724 31. Liu, K., Cui, M. Y., Cao, P., Wang, J. B. Iterative Bayesian Estimation of Travel Times on Urban
725 Arterials: Fusing Loop Detector and Probe Vehicle Data. *PLoS ONE*. **11** (6), e0158123 (2016).
726 32. Ran, B., Song, L., Zhang, J., Cheng, Y., Tan, H. Using Tensor Completion Method to Achieving
727 Better Coverage of Traffic State Estimation from Sparse Floating Car Data. *PLoS ONE*. **11** (7),
728 e0157420 (2016).
729 33. Zhao, J., Li, P., Zhou, X. Capacity Estimation Model for Signalized Intersections under the
730 Impact of Access Point. *PLoS ONE*. **11** (1), e0145989 (2016).
731 34. Wei, X., Xu, C., Wang, W., Yang, M., Ren, X. Evaluation of average travel delay caused by
732 moving bottlenecks on highways. *PLoS ONE*. **12** (8), e0183442 (2017).
733 35. American Association of State and Highway Transportation Officials (AASHTO). *Highway*
734 *Capacity Manual 6th edition*. Washington, D.C. (2010).
735 36. Wang, Y., Qu, W., Ge, Y., Sun, X., Zhang, K. Effect of personality traits on driving style:
736 Psychometric adaption of the multidimensional driving style inventory in a Chinese sample. *PLoS*
737 *ONE*. **13** (9), e0202126 (2018).
738 37. Shen, B., Qu, W., Ge, Y., Sun, X., Zhang, K. The relationship between personalities and self-
739 report positive driving behavior in a Chinese sample. *PLoS ONE*. **13** (1), e0190746 (2018).
740 38. American Association of State and Highway Transportation Officials (AASHTO). *A policy on*
741 *geometric design of highways and streets 6th Edition*. Washington, D.C. (2011).

742 39. Ashraf, M. I., Sinha, S. The "handedness" of language: Directional symmetry breaking of sign
743 usage in words. *PLoS ONE*. **13** (1), e0190735 (2018).
744 40. Lu, A. T., Yu, Y. P., Niu, J. X., John, X. Z. The Effect of Sign Language Structure on Complex
745 Word Reading in Chinese Deaf Adolescents. *PLoS ONE*. **10** (3), e0120943 (2015).
746 41. Fan, L., Tang, L., Chen, S. Optimizing location of variable message signs using GPS probe
747 vehicle data. *PLoS ONE*. **13** (7), e0199831 (2018).

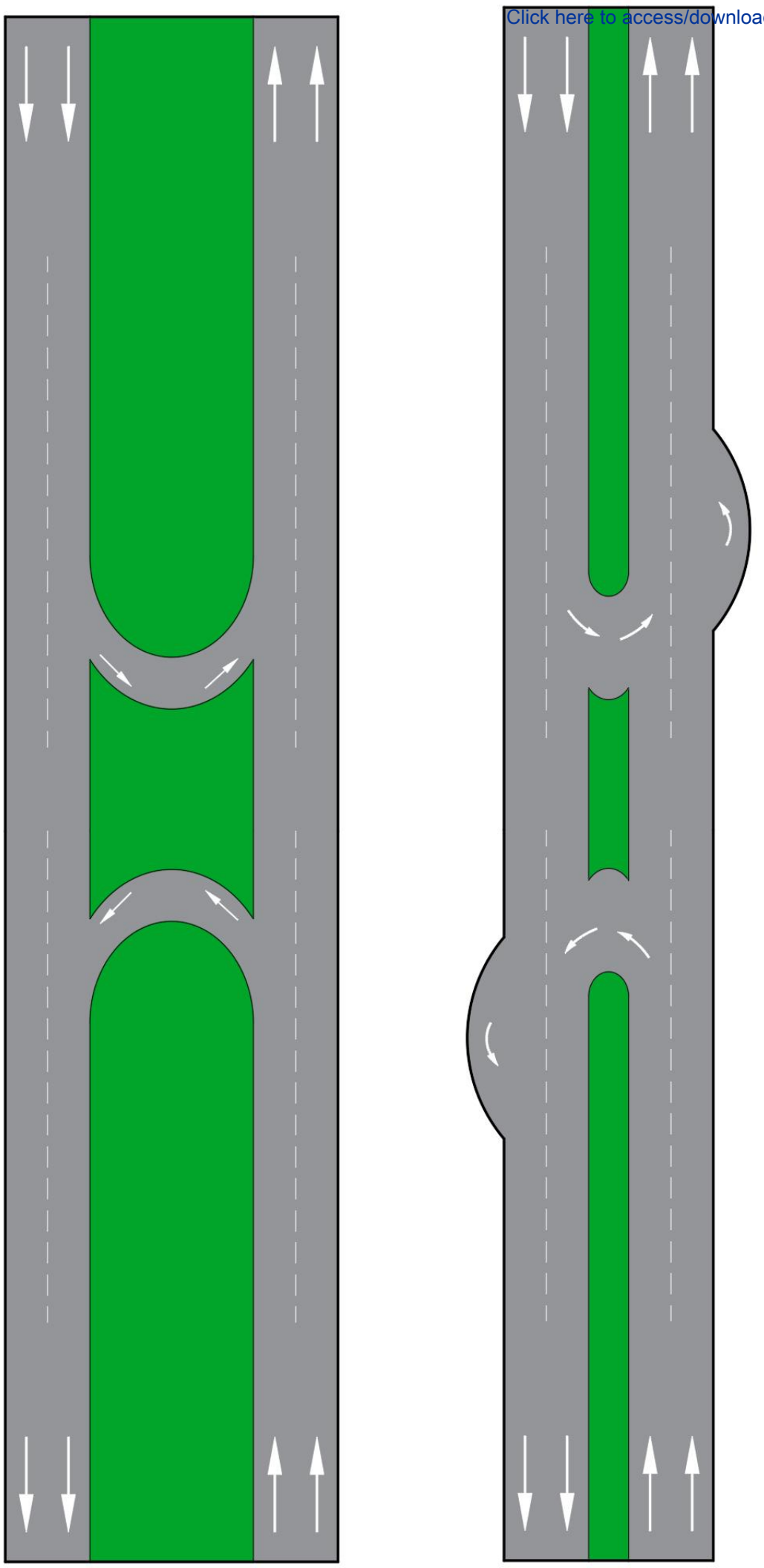

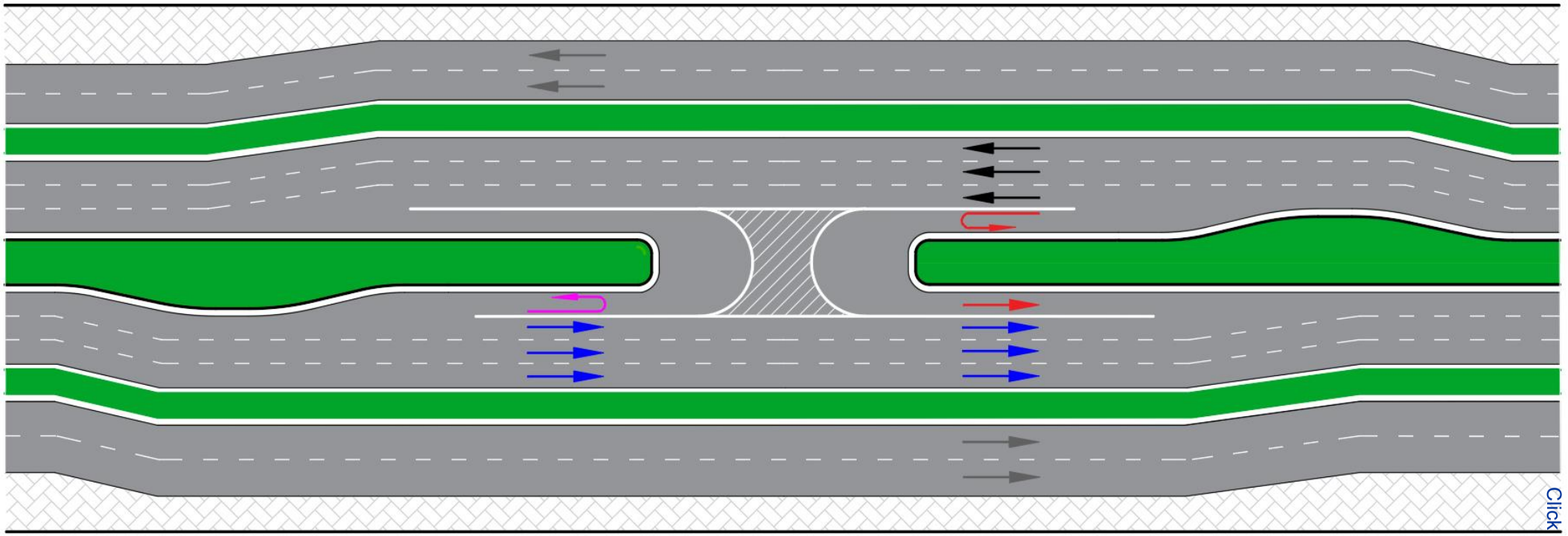

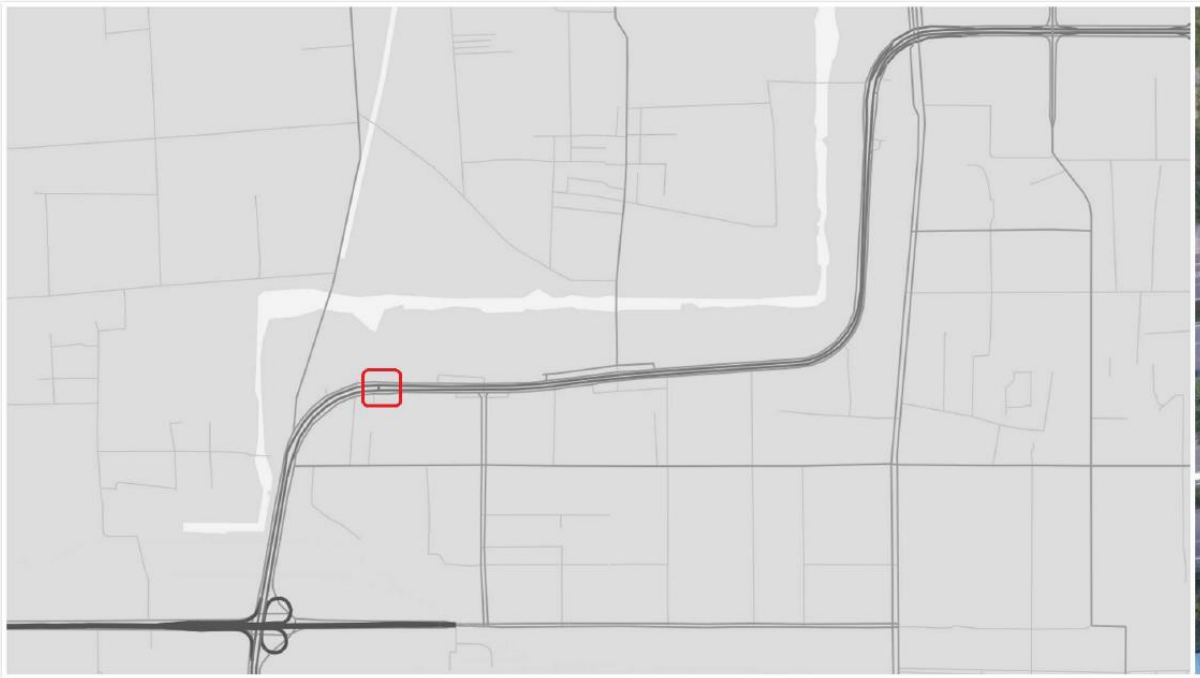

(a)

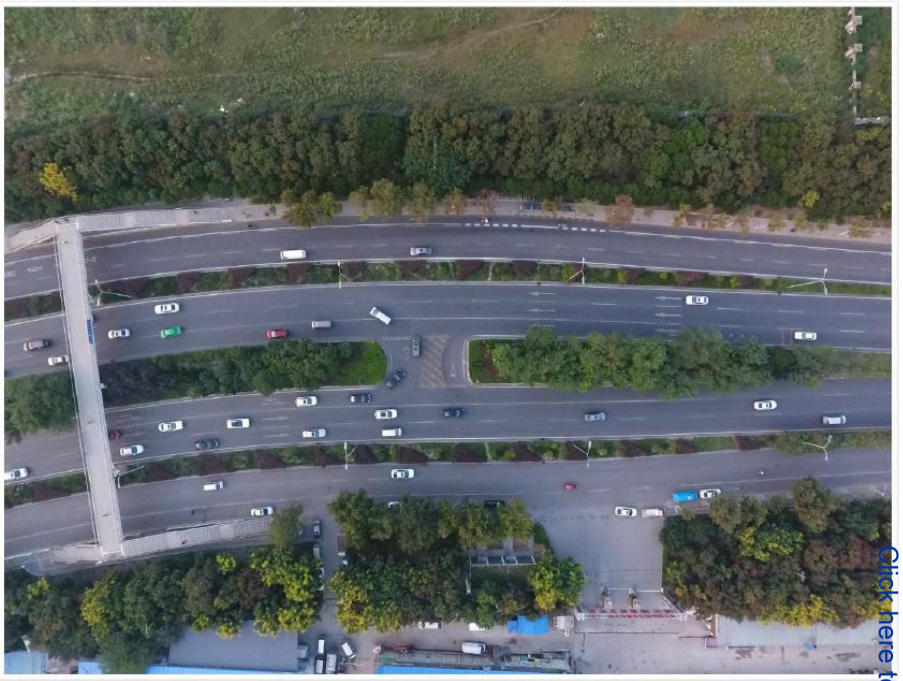

(b)

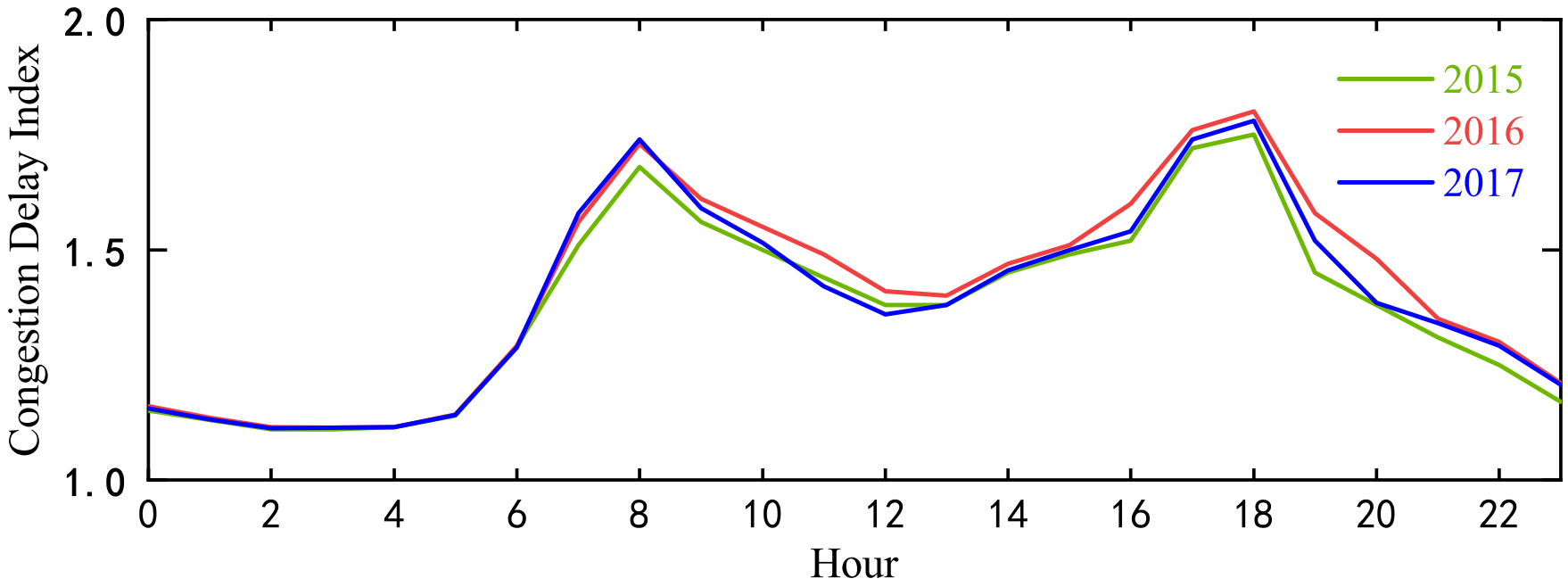

(a)

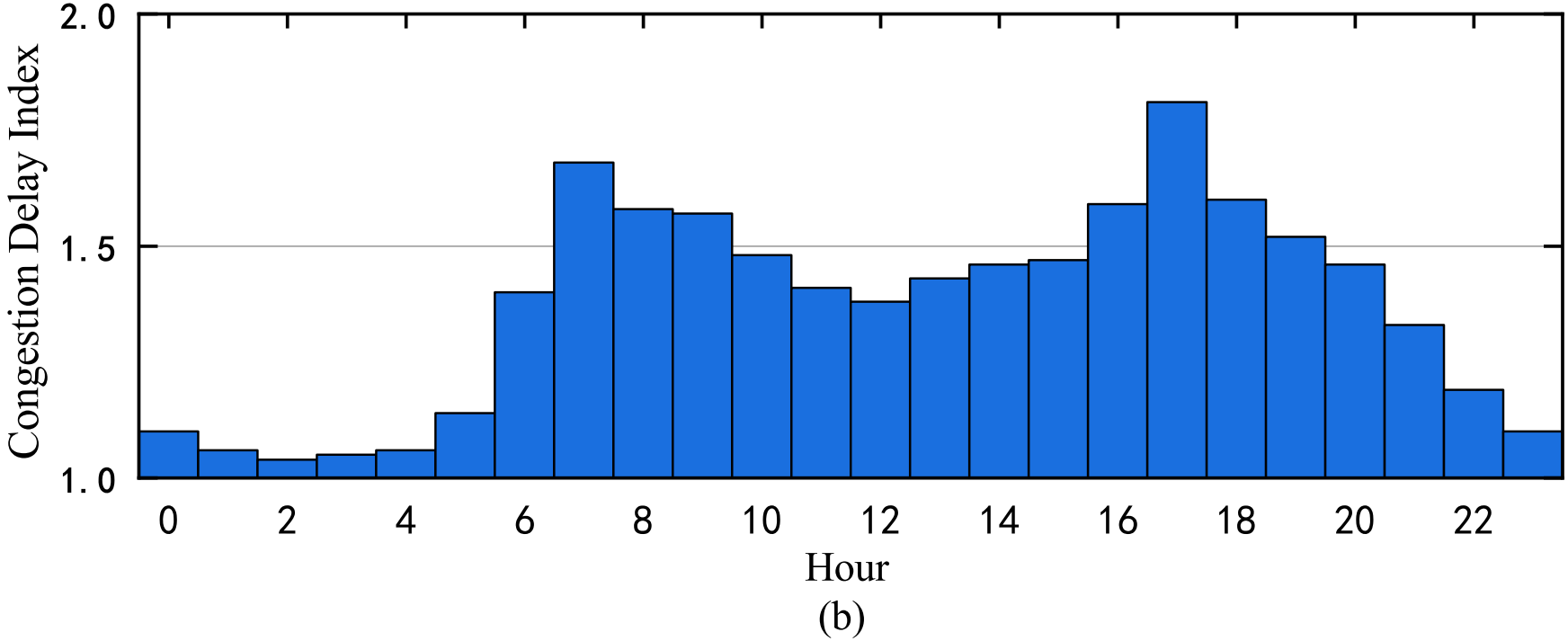

(b)

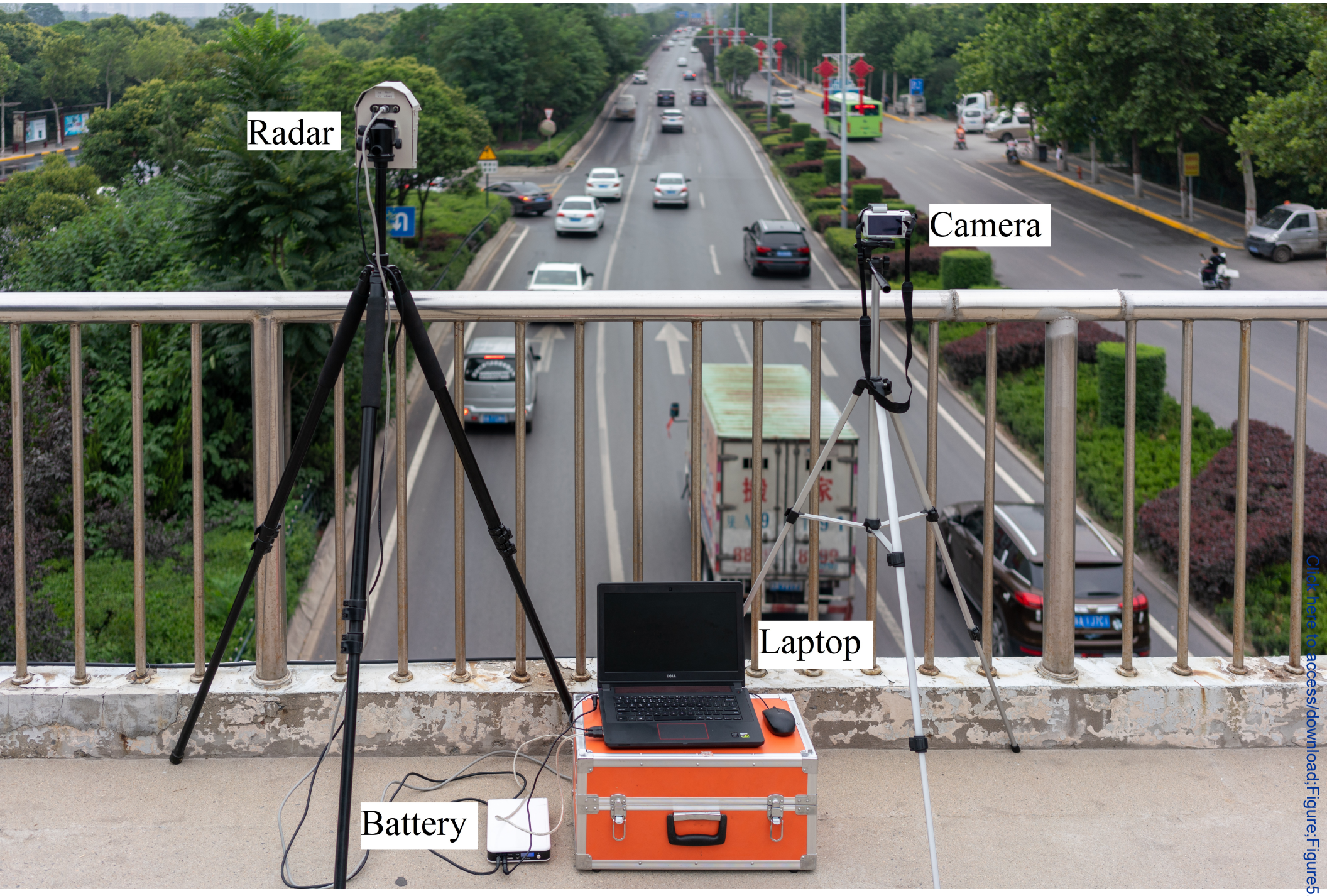

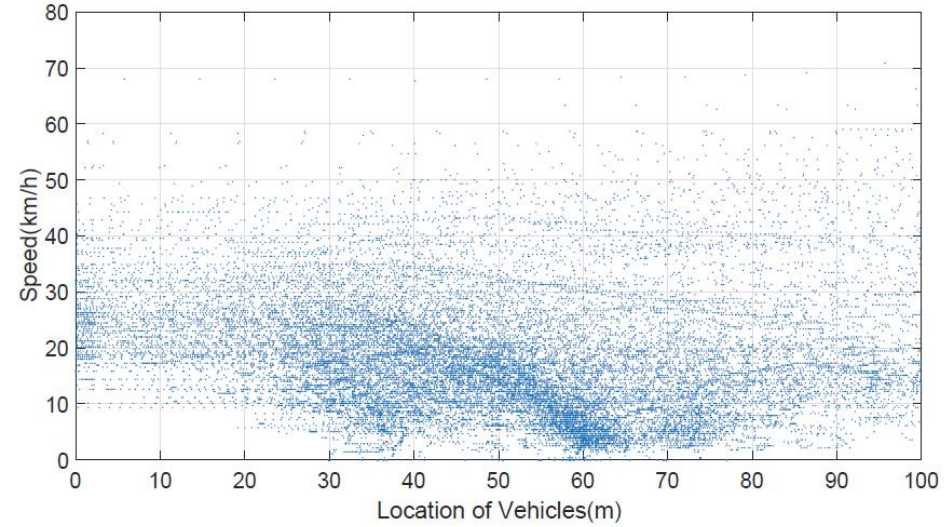

(a)

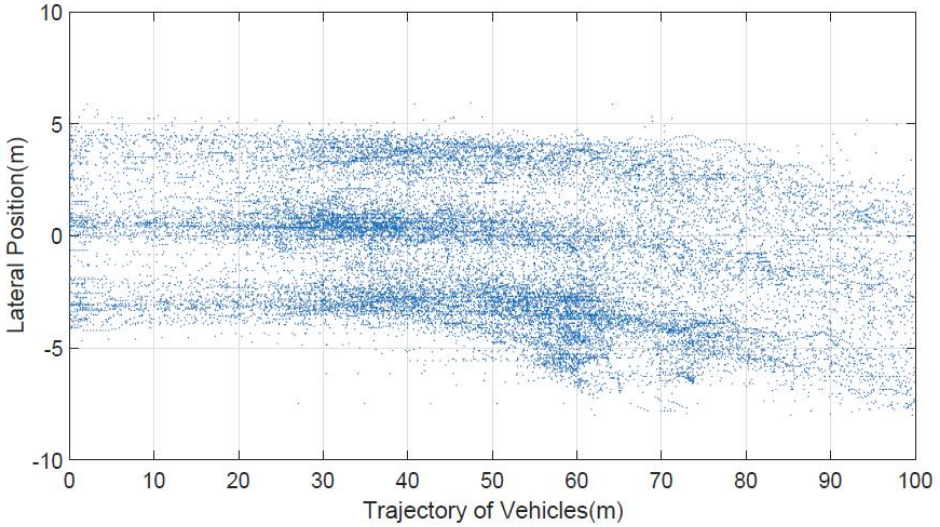

(b)

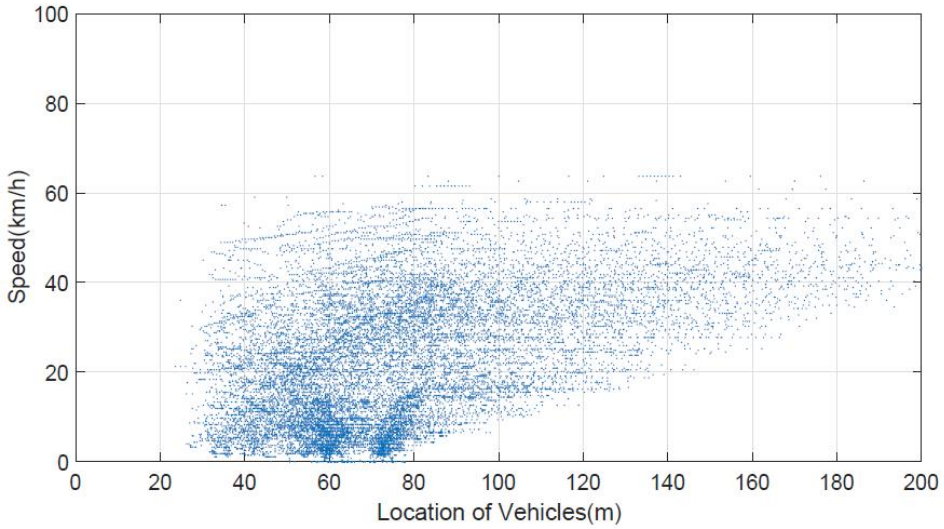

(c)

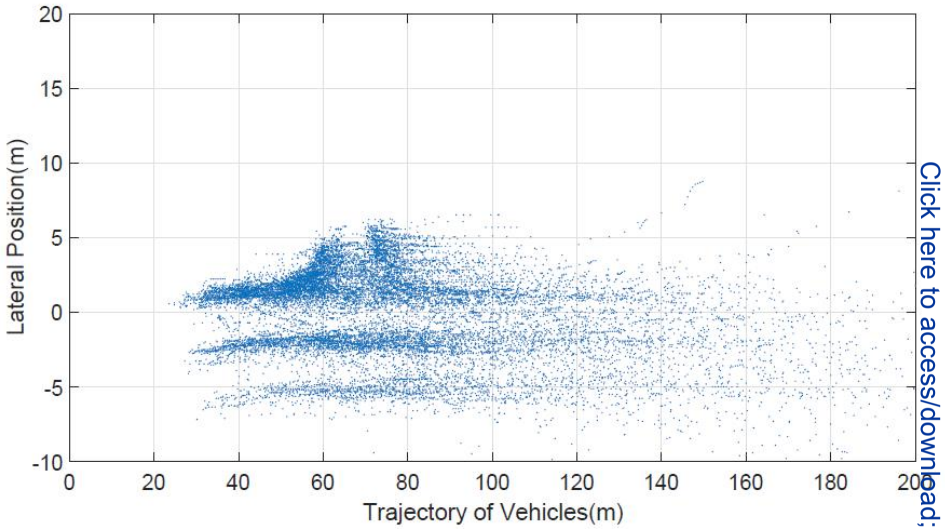

(d)

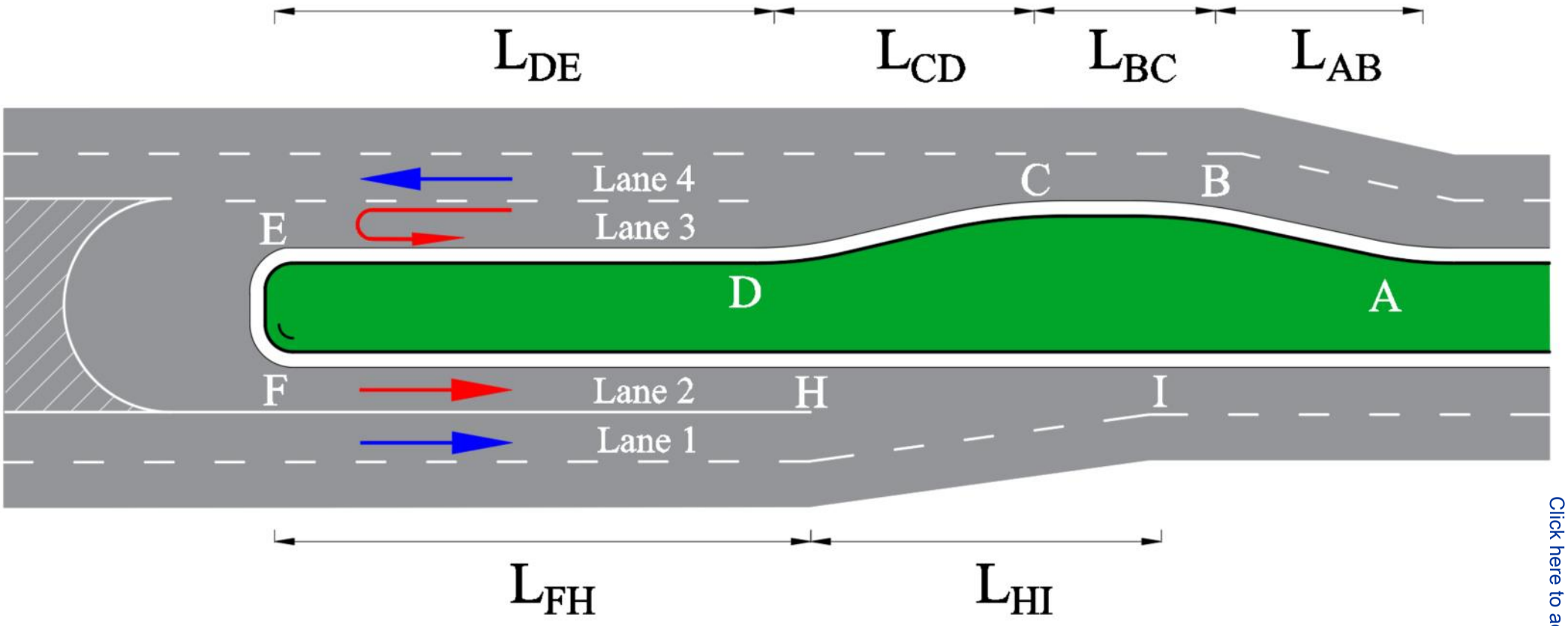

straight through vehicles U-turn vehicles

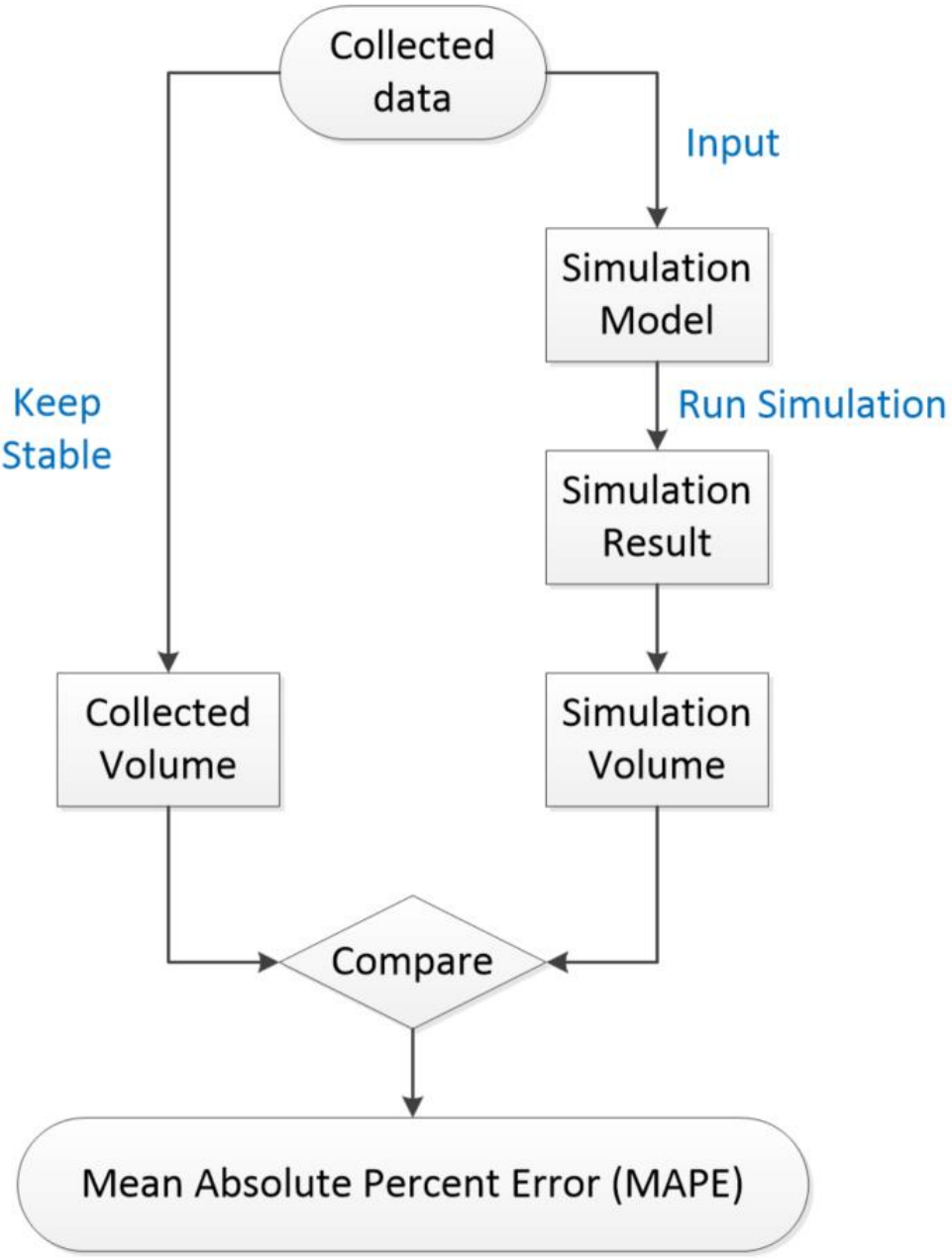

(a)

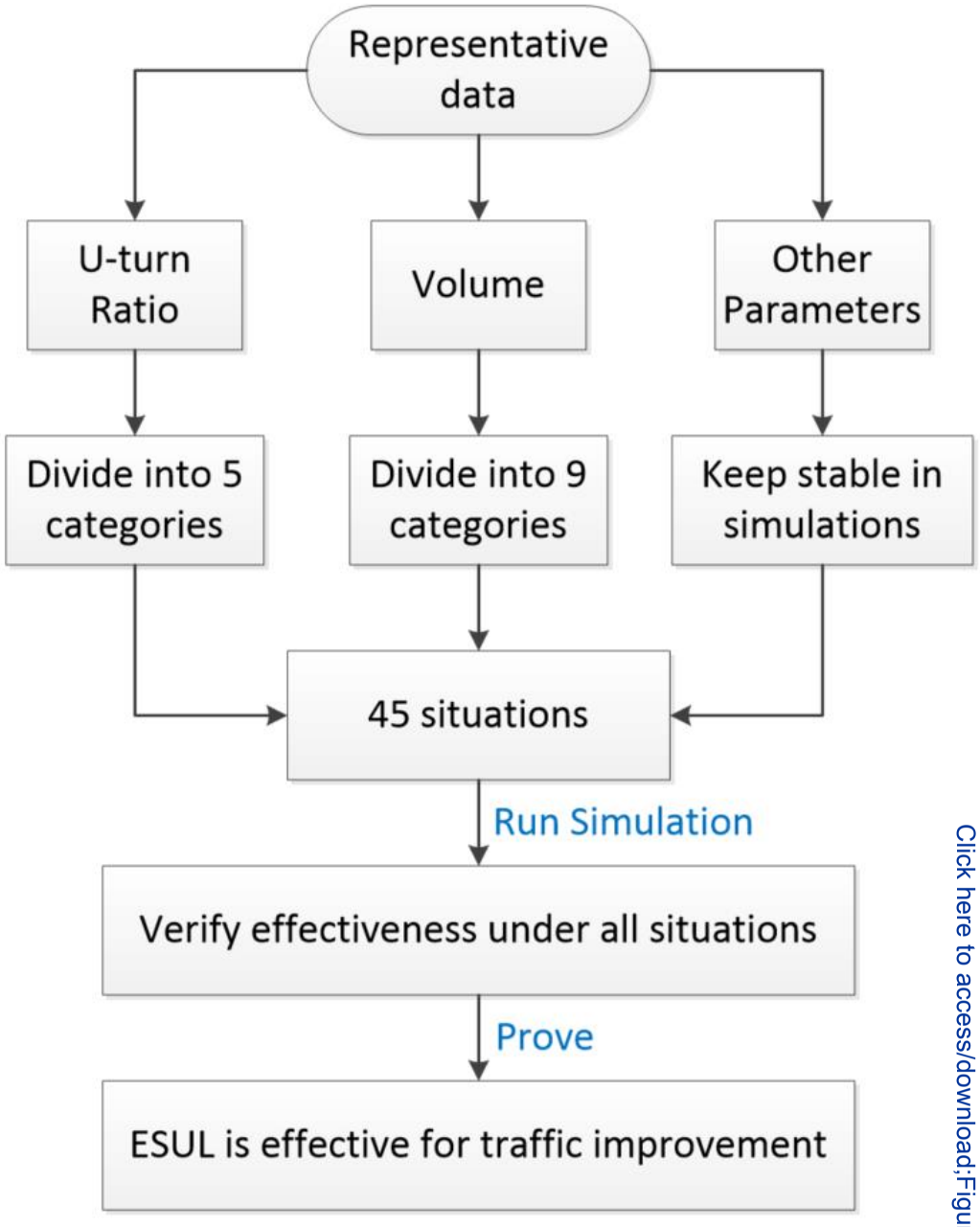

(b)

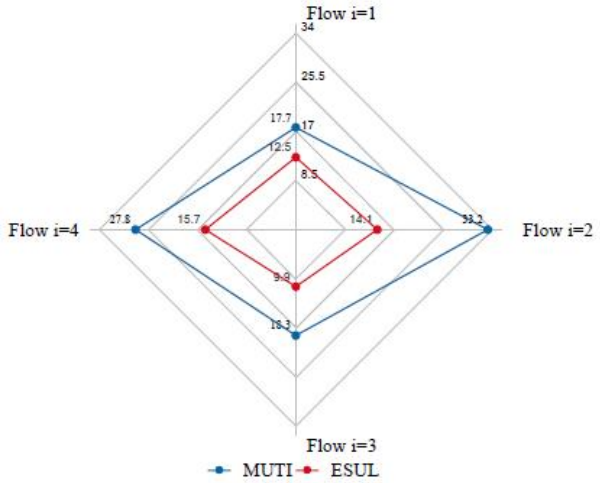

(a)

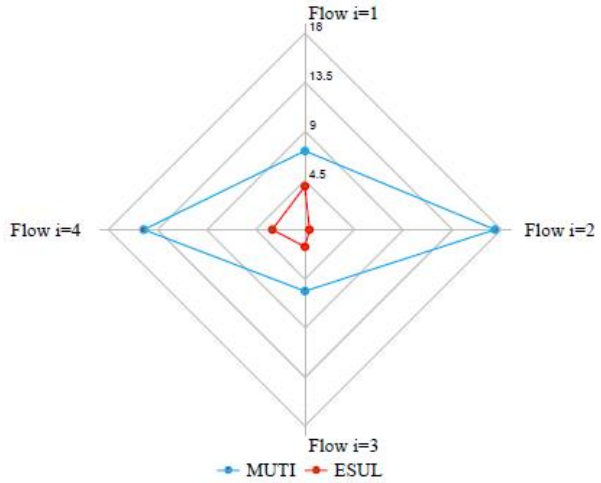

(b)

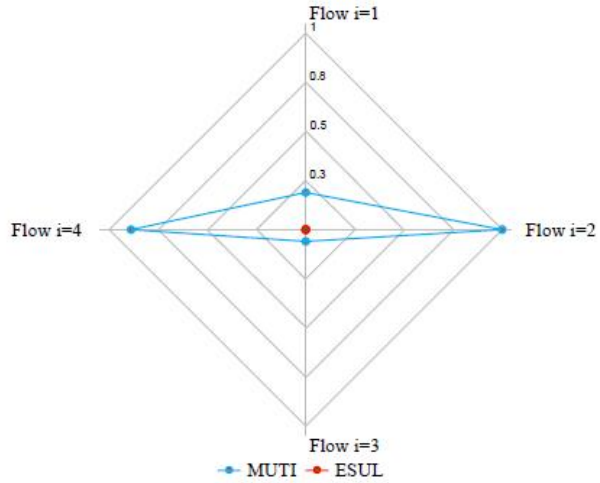

(c)

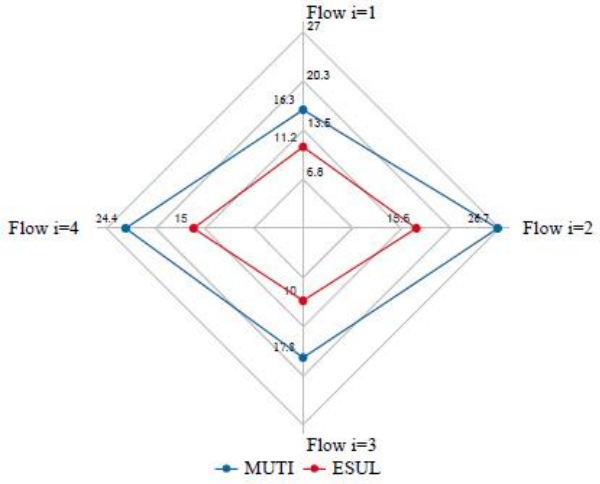

(d)

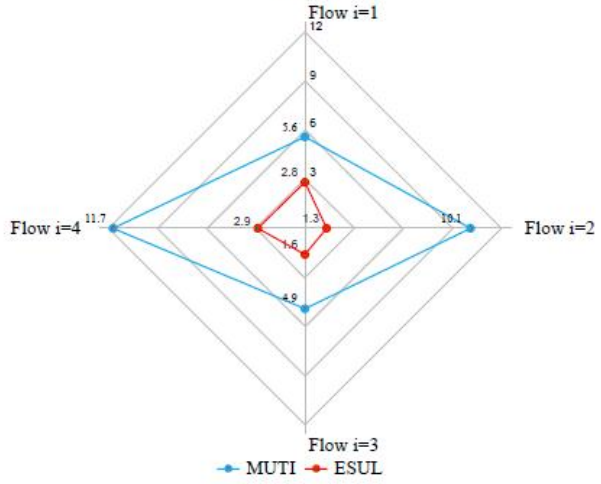

(e)

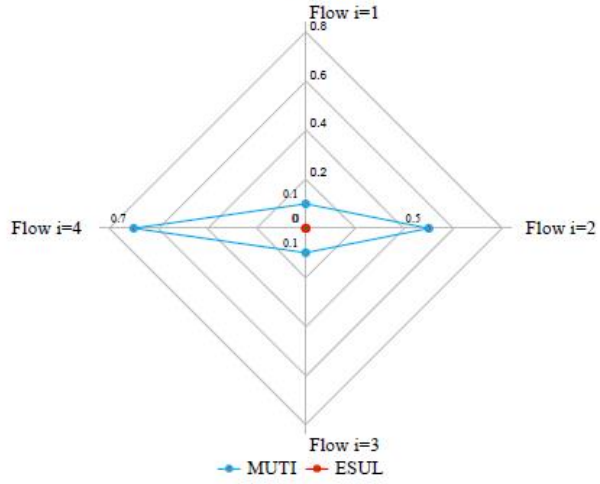

(f)

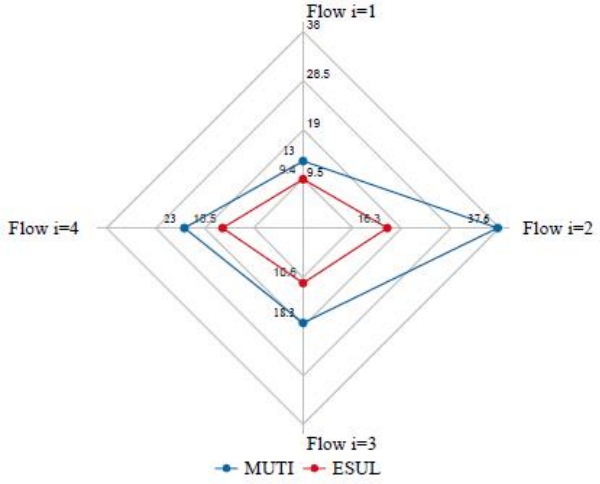

(h)

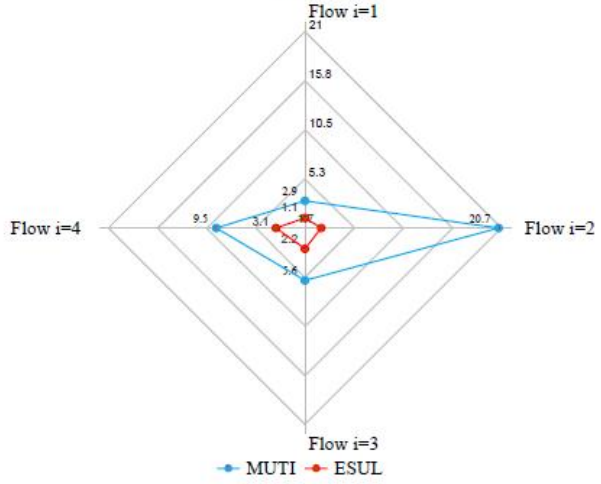

(i)

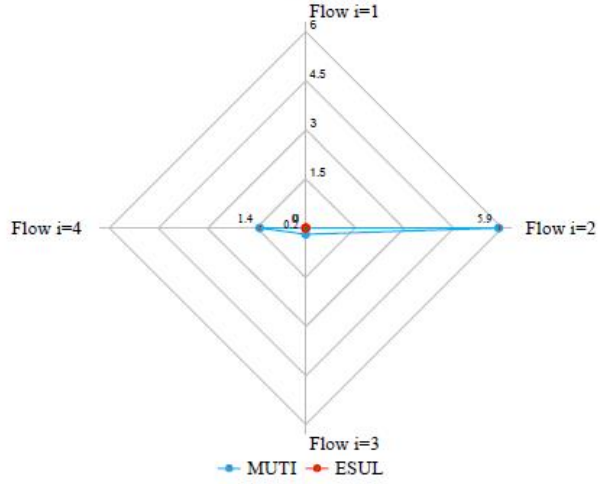

(j)

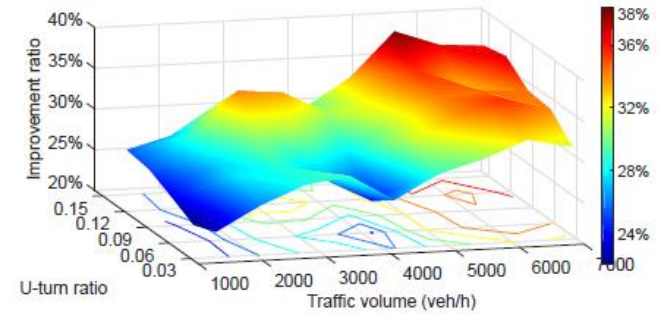

(a)

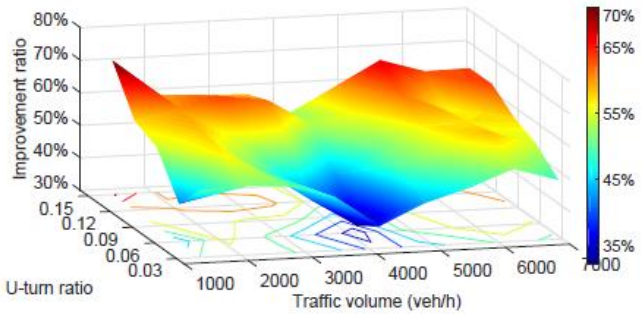

(b)

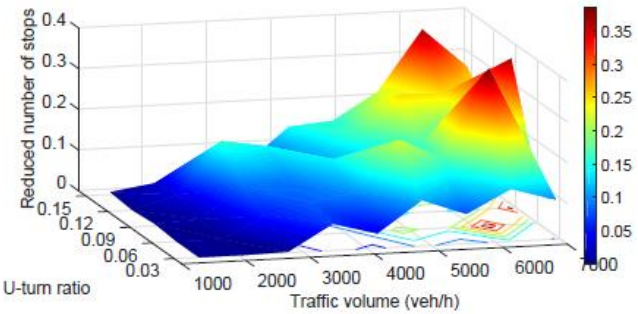

(c)

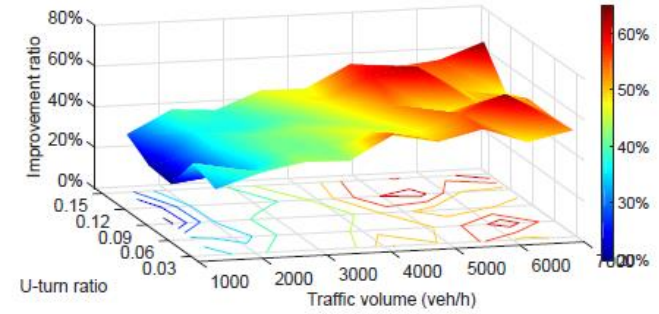

(d)

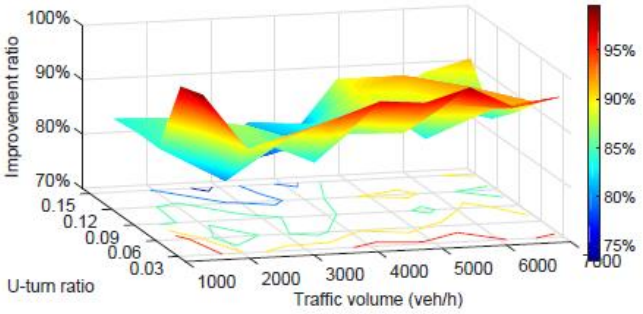

(e)

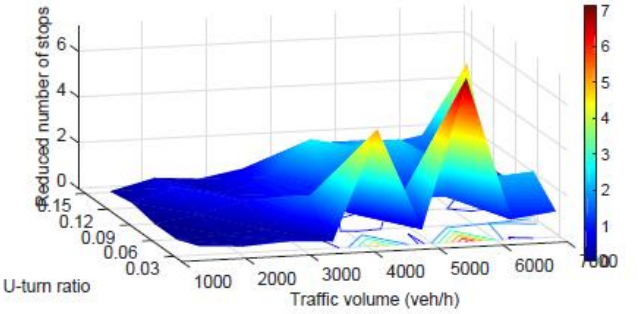

(f)

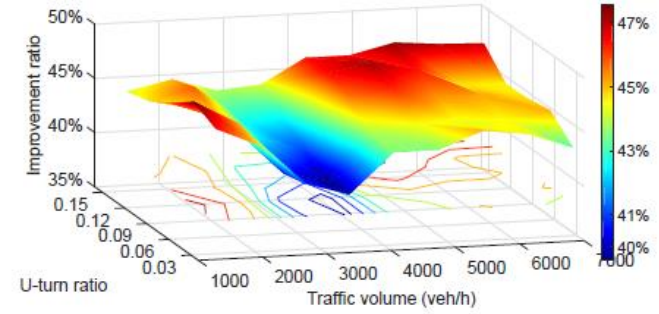

(h)

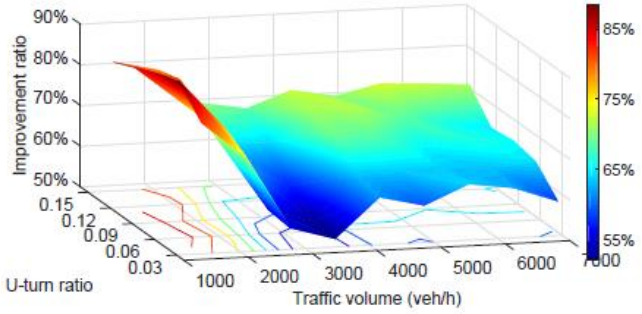

(i)

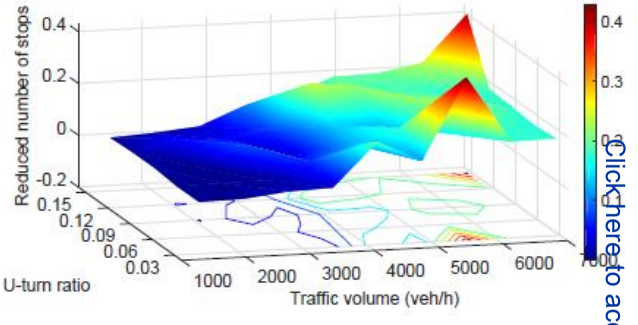

(j)

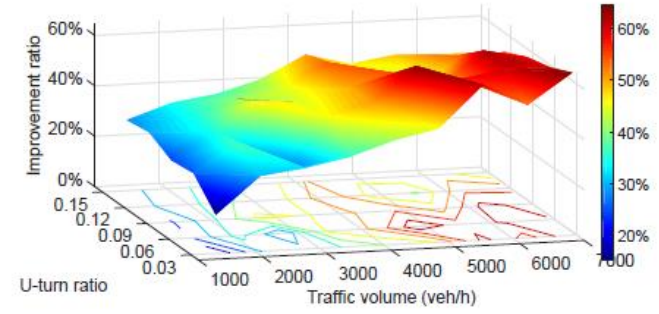

(k)

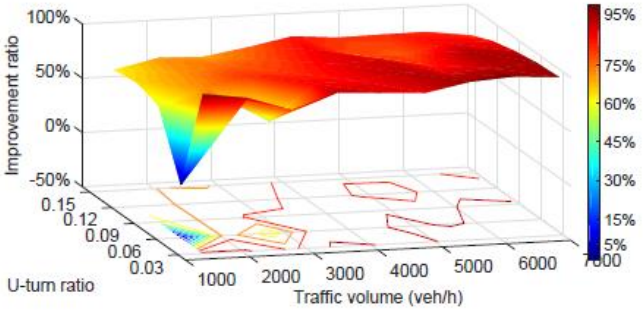

(l)

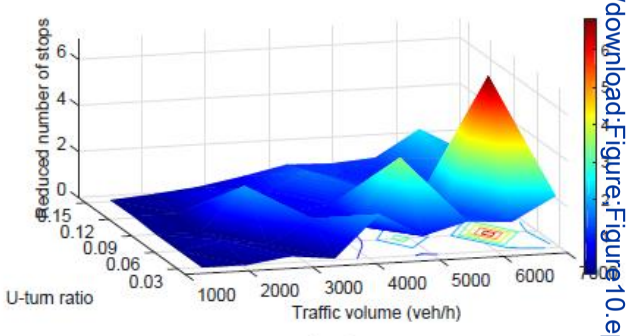

(m)

Table 1

Item	Morning (07:00–08:00)				Middle Noon (13:00–14:00)				E
Direction	EW		WE		EW		WE		EV
Flow	i = 1	i = 2	i = 3	i = 4	i = 1	i = 2	i = 3	i = 4	i = 1
Car	4195	172	3442	504	3001	176	2460	402	1665
Truck	86	10	56	16	79	7	60	41	11
U-turn Ratio	4281:182		3498:520		3080:183		2520:443		1676
Aver. Speed	21.5	11.5	22.2	10.5	36.7	12.3	23.7	11.8	29.3
Max. Speed	73.8	13.4	63.7	12.8	90.4	15.6	75.9	13.5	76.7
Min. Speed	0	0	0	0	0	0	0	0	0

vening (17:00−18:00)		
W	WE	
i = 2	i = 3	i = 4
287	3296	394
6	38	35
:293	3334:429	
12.8	22.9	12.1
14.6	63.7	13.3
0	0	0

Table 2

Item	Description
L_{AB}	166 m. Length for all flows to move outward slightly
L_{BC}	185 m. Length for flow i = 4 to recognize the U-turn sign and take action
L_{CD}	50 m. Diversion length to separate flow i = 3 and flow i = 4
L_{DE}	42 m. Flow i = 4 deceleration length
L_{EF}	Radius = 7.26 m. U-turn width for passenger cars
L_{FH}	180 m. Acceleration length of flow i = 4
L_{HI}	140 m. The length to seek a headway for flow i = 4 and merge into flow i = 1

Table 3

Item	Morning (07:00–08:00)				Noon (13:00–14:00)				Evening (17	
Direction	EW		WE		EW		WE		EW	
Flow	i = 1	i = 2	i = 3	i = 4	i = 1	i = 2	i = 3	i = 4	i = 1	i = 2
Investigated Capacity (veh/h)	4281	182	3498	520	3080	183	2520	443	1676	293
Simulated Capacity (veh/h)	4115	127	3571	501	3000	169	2484	360	1814	268
Individual MAPE (%)	-3.9	-30.2	2.1	-3.6	-2.6	-7.4	-1.4	-18.7	8.2	-8.5
MAPE (%)	-9.9				-7.5				-5	

':00−18:00)	
WE	
i = 3	i = 4
3334	429
3381	409
1.4	-4.6
.7	

Table 4

Item	Travel time (s)			Delay (s)			Number of stops		
Flow	MUTI	ESUL	Rate (%)	MUTI	ESUL	Rate (%)	MUTI	ESUL	Rate (%)
i = 1	17.7	12.5	-29.4	7.2	4	-44.4	0.19	0	-100
i = 2	33.2	14.1	-57.5	17.4	0.4	-97.7	1	0	-100
i = 3	18.3	9.9	-45.9	5.6	1.6	-71.4	0.06	0	-100
i = 4	27.8	15.7	-43.5	14.8	3	-79.7	0.89	0	-100

Table 5

Item	Travel time (s)			Delay (s)			Number of stops		
Flow	MUTI	ESUL	Rate (%)	MUTI	ESUL	Rate (%)	MUTI	ESUL	Rate (%)
i = 1	16.3	11.2	-31.3	5.6	2.8	-50	0.1	0	-100
i = 2	26.7	15.6	-41.6	10.1	1.3	-87.1	0.5	0	-100
i = 3	17.8	10	-43.8	4.9	1.6	-67.3	0.1	0	-100
i = 4	24.4	15	-38.5	11.7	2.9	-75.2	0.7	0	-100

Table 6

Item	Travel time (s)			Delay (s)			Number of stops		
Flow	MUTI	ESUL	Rate (%)	MUTI	ESUL	Rate (%)	MUTI	ESUL	Rate (%)
i = 1	13	9.4	-27.7	2.9	1.1	-62.1	0	0	0
i = 2	37.6	16.3	-56.6	20.7	1.7	-91.8	5.9	0	-100
i = 3	18.3	10.6	-42.1	5.6	2.2	-60.7	0.2	0	-100
i = 4	23	15.5	-32.6	9.5	3.1	-67.4	1.4	0	-100

Table 7

Item	Value								
Car/Truck(bus) ratio	4281:182 (EW) / 3498:520 (WE)								
U-turn ratio (%)	0.03/0.06/0.09/0.12/0.15								
V/C	0.2	0.3	0.4	0.5	0.6	0.7	0.8	0.9	1
Volume (veh/h)	1386	2079	2772	3465	4158	4851	5544	6237	6930

Table of Materials

Click here to access/download;Table of Materials;JoVE60675_Table_of_Materials.xlsx

Name of Material/Equipment	Company	Catalog Number
Battery	Beijing Aozeer Technology Company	LPB-568S
Battery Cable	Beijing Aozeer Technology Company	No Catalog Number
Camera	SONY	a6000/as50r
Camera Tripod	WEI FENG	3560/3130
Laptop	Dell	C2H2L82
Matlab Software	MathWorks	R2016a
Radar	Beijing Aozeer Technology Company	SD/D CADX-0037
Radar Software	Beijing Aozeer Technology Company	Datalogger
Radar Tripod	Beijing Aozeer Technology Company	No Catalog Number
Reflective Vest	Customized	No Catalog Number
VISSIM Software	PTV AG group	PTV vissim 10.00-07 student version

Comments/Description

Capacity:3.7v/50000mAh. Two ports, DC 1 out:19v/5A (max),for one laptop. DC 2 out:12v/3A (max), for one radar.
Connect one battery with one laptop.
The videos shot by the cameras were 1080p, which means the resolution is 1920*1080.
The camera tripod height is 1.4m.
Operate Windows 7 basic system.

Corresponding tripods which could connect with radars, the height is 2m at most.

Response of Paper JOVE60675

Journal of Visualized Experiments

Traffic and Road Engineering Center, Highway Academy, Chang'an University, Xi'an, Shaanxi, China, 710061

Yang SHAO, Corresponding Author, Email: shaoyang19901015@outlook.com

Object: Revised version of the article *Evaluating an exclusive spur dike U-turn design with radars collected data and simulation*

by Yang Shao, Hongtao Yu, Huan Wu, Xueyan Han, Xizhen Zhou, Christian G. Claudel, Hualing Zhang, Chen Yang submitted on December 11th, 2019 for publication in Journal of Visualized Experiment.

The authors are very grateful to the editors for their reports sent on December 16th, 2019, and for their careful reading of the article.

Please find our responses to each of the editors' comments below.

Editorial and production comments:

Editorial comments:

Changes to be made by the author(s) regarding the manuscript:

1. Please note that the editor has formatted the manuscript to match the journal's style. Please retain the same. The updated manuscript is attached and please use this version to incorporate the changes that are requested.

   Thank you for the format work and we revised all problems with no change of the format.

2. The language in the manuscript is not publication grade. Please employ professional copy-editing services.

   Thank you for pointing this out and we checked every sentence to avoid mistakes. And we used Letpub in the first version of the paper.

3. Please further increase the homogeneity between the written protocol and the narration in the video (in this case, update the written protocol according to the video). All information in the video should be in the written protocol, but not all information in written protocol needs to be in the video.

   Thank you for pointing this problem. We edited the video and narration sentence by sentence and make sure the homogeneity.

4. Please address specific comments marked in the attached manuscript.

   We responded every comment in the manuscript.

Changes to be made by the author(s) regarding the video:

1. Title card: Please change "RADARS" to "RADAR".

   Thank you for pointing this out and we revised the title card in the video.

2. Please place the "Results" section card from 9:28 to 10:42 (where you start introducing the results obtained).
   Thank you for pointing this out. The “Results” section card showed from 9:27~9:30.

3. Audio track quality: The audio volume is uneven. The interview sections are much too loud and some narration is still too low. Reduce the Interview audio so the peaks of the volume level do not exceed -6 dB, it's too loud as-is.
   Thank you for pointing this out and we eliminated the background noise of the whole video and make the whole narration sounds in a same loudness.

4. Narration editing: @03:15 There is a deep breath after the word "file" here. Try to end the clip sooner. @03:24 There is a very short but audible piece of an audio clip here mistakingly. It sounds like a mid-breath.
   Thank you for pointing this. We eliminated these noise in the revised video.

5. Editing & pacing: @10:53 Please hold on the completed blue line overlay (""EW through"" ... ""WW u-turn"") before moving on. Add another second so we can see it completed before it disappears."
   Thank you for pointing this out and we added more seconds on this screen to make the audience clearly.

The video was uploaded as the link below due to we cannot use dropbox in China. Thank you.

https://c-t.work/s/34cc6cb13dc043

JOVE60675_v5_20191216.mp4, 888.35MB.